https://doi.org/10.46813/2022-139-109

ACCELERATION OF A HIGH-CURRENT PROTON BEAM IN A LINEAR INDUCTION ACCELERATOR AT ITS COMPENSATION BY ELECTRON BEAMS

O.V. Fedorovskaya, V.I. Maslov, I.N. Onishchenko
National Science Center "Kharkov Institute of Physics and Technology", Kharkiv, Ukraine
E-mail: onish@kipt.kharkov.ua

The dynamics of a high-current proton beam in the cusp magnetic field and in the uniform magnetic field of the drift region in the presence of an accelerating field in the cusp region and of two types of compensating electron beams (before and after the cusp) has been studied. It is shown that for the taken beam parameters and magnetic field it is impossible to accelerate a proton beam of the density higher than 10^{12} cm^{-3} with maintaining its initial transverse size and monoenergeticity.

PACS: 41.75.-i, 52.40.Mj, 52.58.Hm, 52.59.-f, 52.65.Rr

INTRODUCTION

The production and acceleration of high-current ion beams is the problem of current interest in several important applications: controlled thermonuclear fusion with magnetic confinement, inertial thermonuclear fusion on heavy-ion beams of a linear induction accelerator (LIA), surface modification of various materials, radiation materials science, etc.

In [1 - 4], numerical simulation using the 2.5D code "KARAT" [5], devoted to charge and current compensation by electron beams of high-density ion beams of an initial energy 36 MeV in the accelerating gap located in the middle part of the cusp magnetic system, was carried out. It is shown that during the acceleration of such ion beam, the compensation by electron beams ensures the preservation of the ion beam transverse dimensions and monoenergeticity.

The similar investigation [6], performed for the injection of high-density ion beams with a lower energy of several hundred kiloelectronvolt, which is typical for existing high-current ion sources (for example, [7]), in the absence of an accelerating field, showed that a threshold arises in beam density 10^{12} cm^{-3}, above which transportation is not possible.

In this paper, the case of [6] is studied but in the presence of an accelerating field in the cusp region. The dynamics of a proton beam in the magnetic field of a cusp configuration and in the uniform magnetic field of the drift region with compensation by the axial electron beam, injected into the first half of the cusp, and by the electron beam, injected along the radius into the second half of the cusp, is studied depending on the beam density.

The dynamics of the proton beam is considered for the cases of the high (3.4 T) and low (0.34 T) magnetic fields in order to determine the degree of magnetic isolation of electrons before the acceleration of the proton beam and its compensation after it left the accelerating gap.

1. PROBLEM FORMULATION

The studies were carried out using 2.5-dimensional numerical simulation in rz-geometry (Fig. 1). In considering model, the computational region consists of accelerating and drift parts. The magnetic field is created by two coils with opposite currents (to create so called "casp") and a solenoid (to create drift region of the uniform magnetic field). It is followed by another cusp in the case of a multisectional induction accelerator.

Two values of magnetic field are taken B_0 = 3.4 and 0.34 T. The length of the system z_L = 50 cm, radius r_L = 7 cm. From the left, tubular proton beam (energy W_i = 240 keV) and the main electron beam (energy W_e = 130 eV) of the same speed ($v_i = v_e$) and density ($n_i = n_e$), with inner and outer radii r_{min} = 0.7 cm, r_{max} = 1.4 cm are injected. Another electron beam (additional one) is radially injected from the periphery uniformly over the azimuth toward the axis into the second half of the cusp. The parameters of this electron beam and the value and the topography of the magnetic field of the cusp are chosen so that transverse sizes and densities of electron and proton beams are coincided in drift region. Three values of the proton beam density $n_i = 10^{10}$, 10^{11}, 10^{12} cm^{-3} are considered. Electric field in the accelerating gap of the length of 1 cm E_z= 240 kV/cm is applied before the middle of the cusp. The distance between the coils is 3 cm.

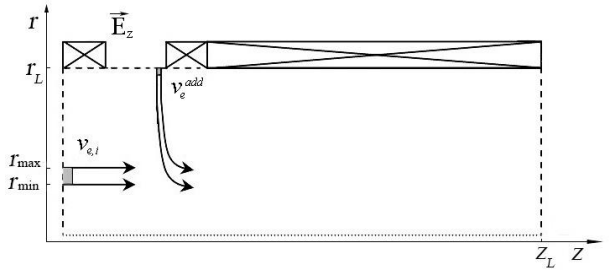

Fig. 1. The magnetic system geometry and the regions of injection of a proton and two electron beams

2. DYNAMICS OF THE PROTON BEAM OF VARIOUS DENSITIES IN THE PRESENCE OF ACCELERATING FIELD

2.1. HIGH MAGNETIC FIELD

The case of the accelerating gap electric field presence in the absence of the additional electron beam.

The results obtained in a high magnetic field are given for a time instant of 70 ns, when the stationary regime has already achieved.

For the density of the proton and electron beams $n_i = n_e = 10^{11}$ cm^{-3}, as it can be seen from Fig. 2,a, in the

absence of an accelerating field the electron beam moves along the magnetic field lines and drags along the essential part of the ion beam to the periphery. It means that electrons are magnetized enough to follow up the magnetic field lines. As for the njn magnetized proton beam of such density it is influenced more by the polarization field strong enough to change its rectilinear motion.

In the presence of an accelerating field (see Fig. 2,b), the electron beam is reflected from the accelerating gap, and the ion beam gets into the accelerating gap and is accelerated and passes through the cusp. But similarly to simple transportation of the ion beam (see Fig. 2,a and [6]) in the drift region it "inflates" due to its drift in crossed electric and magnetic fields that looks like beam corrugation. So the accelerating field does not allow avoiding the increase of ion beam transverse size.

For the density of the proton and electron beams $n_i = n_e = 10^{12}$ cm^{-3} (see Fig. 2,c,d) electron beam drags along almost the whole ion beam to the periphery with or without accelerating field.

The case of the presence both the accelerating gap electric field and the additional electron beam.

At the density of the proton beam $n_i = 10^{10}$ cm^{-3}, as well as in the accelerating field absence in a strong magnetic field [6], the following particle dynamics arises. In the radial electric field of space charge and polarization field and the longitudinal external magnetic field the complicated motion of protons occurs. Resulting azimuthal drift of the proton beam is observed as its periodic corrugation along the drift region (Fig. 3,a).

Energy gain of the proton beam is corresponded to the accelerating field (total proton beam energy after the cusp W_i = 480 keV), that retains along the drift region (see Fig. 3,b).

The main electron beam does not reach the cusp under the influence of the electric field in accelerating gap and the space charge field of the additional electron beam. This occurs both at low ($n_i = 10^{10}$cm^{-3}) and high ($n_i = 10^{12}$ cm^{-3}) proton beam densities.

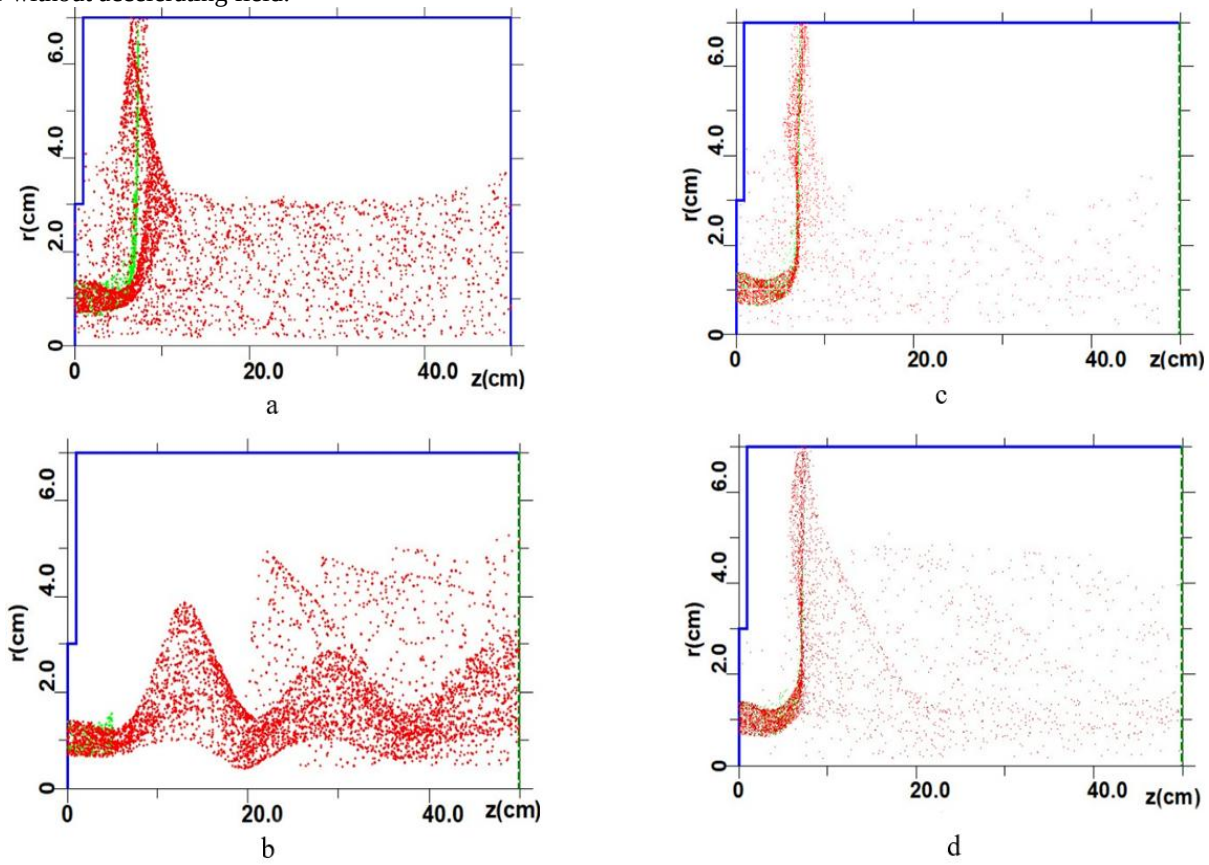

Fig. 2. Arrangement of particles of the proton (red) beam and main electron (green) beam, in the absence of an additional electron beam, on the rz-plane: (a, c) accelerating field is absent; (b, d) accelerating field is applied; (a, b) – $n_i = 10^{11}$ cm^{-3}; (c, d) – $n_i = 10^{12}$ cm^{-3}

The proton beam with density $n_i = 10^{11}$ cm^{-3} diverges in the cusp more strongly, since space charge fields are greater. In the drift region the periodic corrugation of the proton beam occurs (see Fig. 3,c) with amplitude greater than at the density $n_i = 10^{10}$ cm^{-3}. Beside for density $n_i = 10^{11}$ cm^{-3}, the proton beam is accelerated not only by the electric field in the accelerating gap, but also by the increased space charge field of the additional electron beam after cusp (see Fig. 3,d). The decrease in the velocity of the additional electron beam along the magnetic field line at the end of the cusp occurs due to the rearrangement of the radial motion of electrons into a longitudinal one, and therefore the density of the additional beam in this place becomes higher. Behind the region of increased space charge of the additional electron beam, the latter is accelerated, and the proton beam slows down, finally having energy W_i = 480 keV at the system exit.

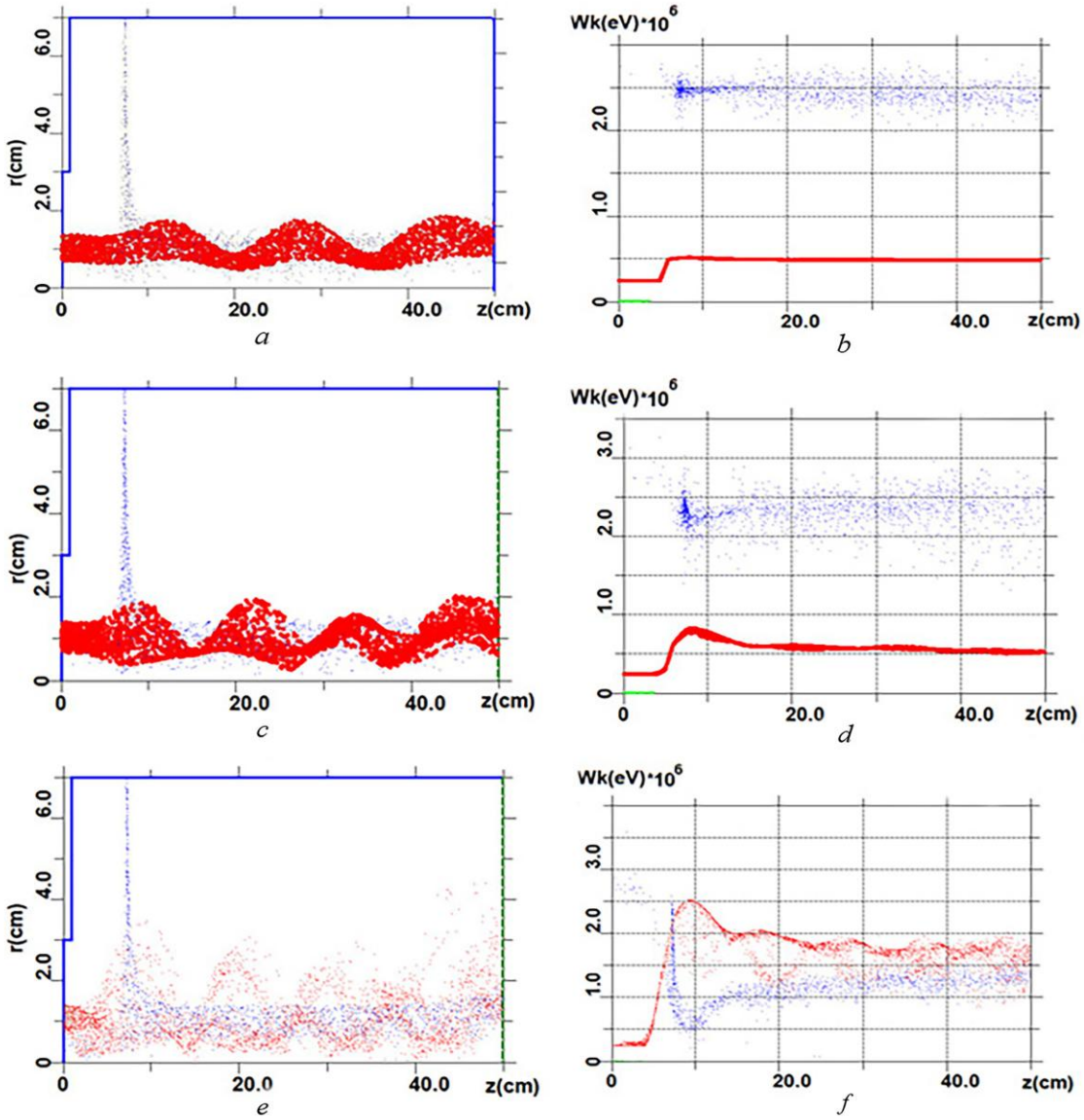

Fig. 3. Arrangement of particles of the proton (red) beam, main electron (green), and additional electron (blue) beams, on rz-plane (a, c, e). Kinetic energy of particles of the proton beam, main electron and additional electron beams vs the longitu dinal coordinate z (b, d, f). (a, b) – $n_i = 10^{10}$ cm^{-3}; (c, d) – $n_i = 10^{11}$ cm^{-3}; (e, f) – $n_i = 10^{12}$ cm^{-3}

At proton beam density $n_i = 10^{12}$cm^{-3}, its corrugation amplitude is greater (see Fig. 3,f) than in the first two cases, that leads to an increase in its energy spread. The additional electron beam in the end of the cusp is significantly slowed down to 0.5 MeV, and the proton beam acquires energy of 2 MeV due to the space charge of the additional beam and 0.24 MeV in the accelerating electric field (see Fig. 3,f). Further in the drift gap, the proton beam slows down, while the additional electron beam accelerates. At the system exit, the energy of the proton beam is about 2 MeV, since the proton beam accelerated due to two factors: the electric field in the cusp and the space charge field of additional electron beam.

However, as in the absence of an accelerating field [6], both compensating electron beams do not allow maintaining the transverse dimensions of the proton beam after acceleration in the cusp and transport in the drift region to the next section.

2.2. LOW MAGNETIC FIELD

Since the magnetic field magnitude changes the particle dynamics, in this subsection options for accelerating a proton beam with densities $n_i = 10^{10}$ cm^{-3} and $n_i = 10^{12}$ cm^{-3} are considered for low magnetic fields, the influence on particles of which is not so significant as for $B_0 = 3.4$ T.

In contrast to the case when there is no accelerating field, and the magnetic field is $B_0 = 3.4$ T [5], in a the main electron beam, a high-current proton beam ($n_i = 10^{12}$ cm^{-3}) is not dragged along the magnetic field lines by the main electron beam to the periphery, and passes into the drift region together with the electron beam (see Fig. 4,a-d), despite the electric field, decelerating the electrons (Fig. 4,a). In this case, the electrons of the main beam, reaching the cusp, lag behind the ions and slightly diverge in the radial direction. As a result, a polarization field arises between the ions and lagging

electrons. When the longitudinal component E_z of this field reaches the threshold value, the proton beam drags the electron beam due to the polarization field (see Fig. 4,a-c). The electrons of the main electron beam (green) are accelerated and pass through the cusp, while the protons (red) are decelerated (see Fig. 4,d). In this case, drift in crossed radial electric and longitudinal magnetic fields is observed in the form of corrugation (see Fig. 4,b-c).

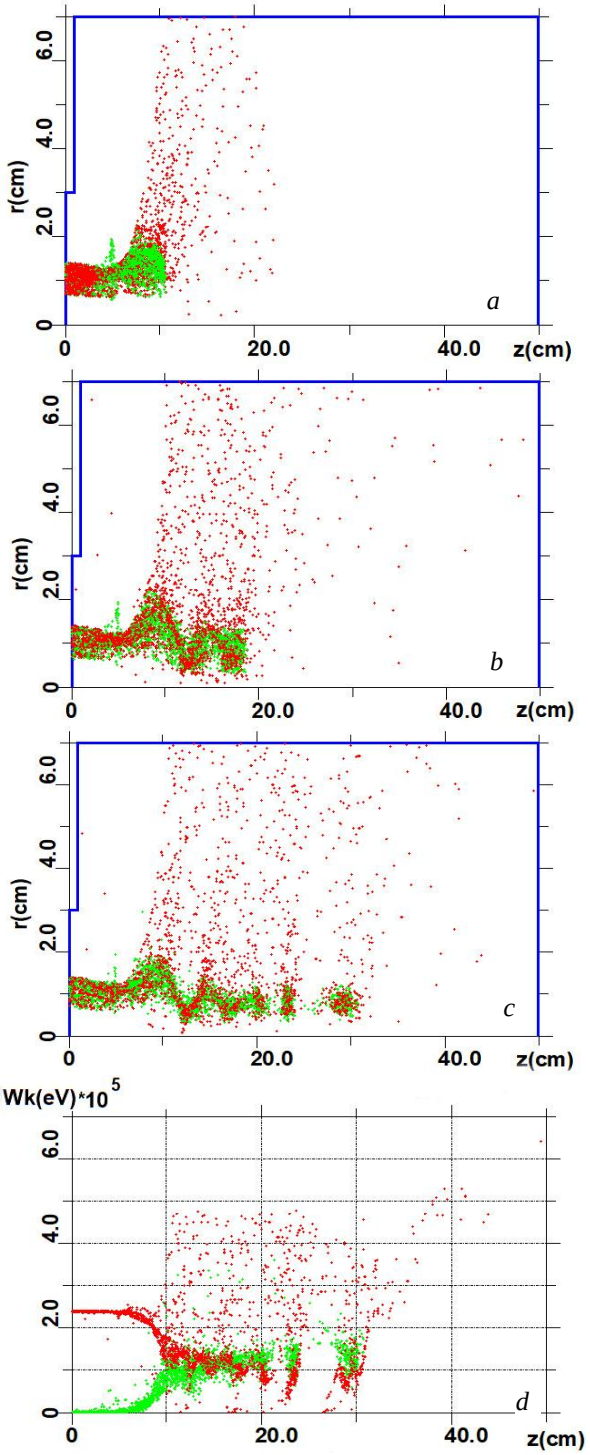

Fig. 4. Arrangement of the particles of the proton (red), main electron (green) beams on the rz-plane at a time of: 20 ns, $n_i = 10^{12}$ cm^{-3} (a); 60 ns, $n_i = 10^{12}$ cm^{-3} (b); 120 ns, $n_i = 10^{12}$ cm^{-3} (c); kinetic energy of the particles of the proton and main electron beams vs the longitudinal coordinate z, $n_i = 10^{12}$ cm^{-3} (d)

At a magnetic field $B_0 = 0.34$ T and the presence of both compensating electron beams in the case of $n_i = 10^{10}$ cm^{-3}, the proton beam dynamics is changed: the corrugation amplitude decreased, and its period increased (Fig. 5,a).

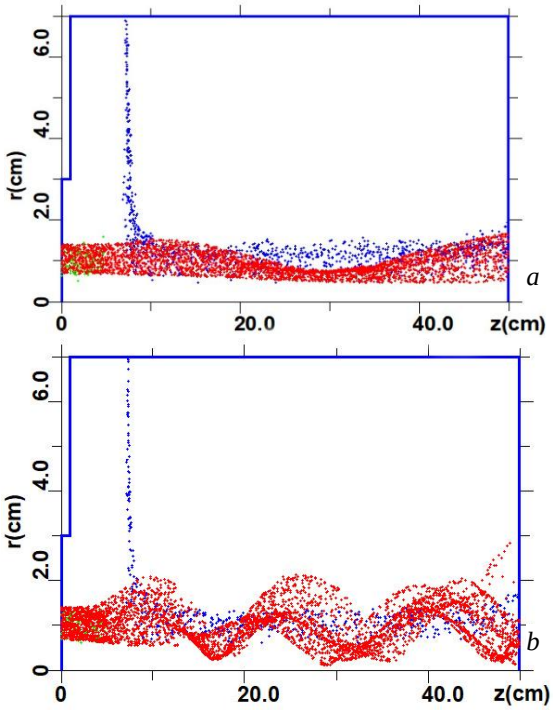

Fig. 5. Arrangement of the particles of the proton (red), main electron (green) and the additional electron (blue) beams on the rz-plane. $n_i=10^{10}$ cm^{-3} (a); $n_i=10^{11}$ cm^{-3} (b)

A proton beam with density $n_i = 10^{11}$ cm^{-3} in a low magnetic field has a larger corrugation amplitude (see Fig. 5,b) than in a high magnetic field (see Fig. 3,c).

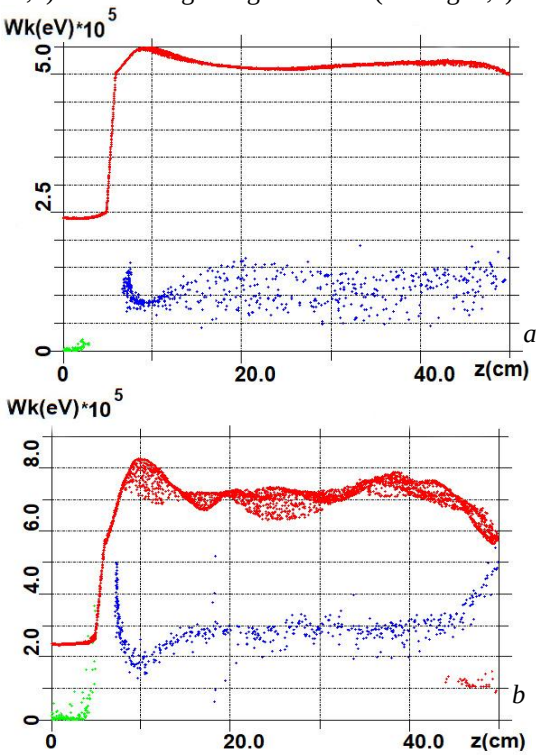

Fig. 6. Kinetic energy of the proton (red), main electron (green) and additional electron (blue) beams vs the longitudinal coordinate z. $n_i=10^{10}$ cm^{-3} (a); $n_i=10^{11}$ cm^{-3} (b)

Wherein, a proton beam with a density $n_i = 10^{10}$ cm^{-3} is accelerated in the electric field, having energy about 500 keV at the cusp exit (Fig. 6,a). The proton beam with a density of $n_i = 10^{11}$ cm^{-3} is accelerated due to both the electric field and the space charge field of the additional electron beam ($W^{add} = 0.5$ MeV), which made it possible to obtain its energy of about 600 keV at the system exit (see Fig. 6,b).

At density of 10^{12} cm^{-3}, the proton beam "scatters" in the drift region (therefore is not presented), because it is not compensated by a radially injected electron beam. The proton and electron beams have been moved apart in space – the electron beam moves along the magnetic field lines, and the proton beam "sweepingly" drifts in crossed radial electric and external longitudinal magnetic fields, reaching the walls of the chamber. Thus, in the considered case of a weak magnetic field, there exists a density threshold, when compensation becomes impossible.

CONCLUSIONS

Dynamics of a high-current proton beam in a magnetic cusp with an accelerating gap and in an uniform magnetic field of drift region, using charge and current compensation before entering the accelerating gap by an axial electron beam, injected into the first half of the cusp, and after leaving the accelerating gap by an electron beam, injected along radius to the second half of the cusp, was studied depending on the density of the proton and electron beams. Such a scheme is of interest as an injector, in particular, in the problem of heavy-ion inertial fusion using a high-current ion beam of LIA.

The results of numerical simulation show that for all considered beam densities (10^{10}…10^{12}cm^{-3}) corrugation of the tubular proton beam occurs in the drift region, caused by proton drift in the crossed longitudinal external magnetic field and the radial electric field of uncompensated beams. This leads to an increase in transverse dimensions and energy spread, in contrast to the results of [1-4], and to the similar dynamics for simple proton beam transport without acceleration [6]. The threshold density of the proton beam, for which it becomes unsuitable for injection into the subsequent accelerating section, remains the same 10^{12} cm^{-3}, as in [6].

In a low magnetic field the dynamics of deterioration in the quality of the proton beam in the scheme under consideration is more obvious and there is the density threshold too. This is due to the weakening of the magnetic isolation of electrons at lower magnetic fields. For the same reason, in a lower magnetic field, two phenomena that are not foreseen by the idea under study of compensation by two electron beams arise. First, the axial beam is dragged by the proton beam into the accelerating gap. Secondly, the proton beam, in addition to acceleration in an external electric field, experiences additional acceleration in the space charge field of the additional radially injected electron beam.

The results, obtained in this paper, force us to reconsider the original concept of ion beam compensation by electron beams or to limit ourselves to an ion beam density lower than 10^{12} cm^{-3}.

REFERENCES

1. V.I. Karas', E.A. Kornilov, O.V. Manuilenko, O.V. Fedorovskaya. Particle dynamics in the injector of ion linear induction accelerator // *Problems of Atomic Science and Technology. Series "Nuclear Physics Investigations"*. 2019, № 6, p. 85-89.
2. V.I. Karas', E.A. Kornilov, O.V. Manuilenko, O.V. Fedorovskaya. Particle dynamics in the injector of ion linear induction accelerator // *Problems of Atomic Science and Technology. Series "Plasma Electronics and New Methods of Acceleration"*. 2008, № 4, p. 83-88.
3. V.I. Karas', N.G. Belova. Acceleration and stability of high-current ion beams in two accelerating gaps of a linear induction accelerator // *Plasma Phys. Rep*. 1997, v. 23, № 4, p. 328-331.
4. V.I. Karas', O.V. Manuilenko, E.A. Kornilov, V.P. Tarakanov, O.V. Fedorovskaya. Dynamics of high-current ion beam in the drift gap of induction accelerator at different variants of charge compensation // *Problems of Atomic Science and Technology. Series "Plasma Physics"*. 2014, № 6, p. 104-107.
5. V.P. Tarakanov. User's Manual for Code KARAT // *Springfield VA: Berkley Research Associates Inc.* 1992, p. 137.
6. I.N. Onishchenko, O.V. Fedorovskaya. Simulation of the compensation of a high-current ion beam by an electron beam in a cusp magnetic system // *Problems of Atomic Science and Technology. Series "Plasma Electronics and New Methods of Acceleration"*. 2021, № 4, p. 122-127.
7. Hiroaki Ito, Yasushi Ochiai and Katsumi Masugata. Development of High-current Pulsed Heavy-ion-beam Technology for Applications to Materials Processing // *Journal of the Korean Physical Society*. 2011, v. 59, № 6, p. 3652-3656.

Article received 12.06.2022

ПРИСКОРЕННЯ СИЛЬНОСТРУМОВОГО ПРОТОННОГО ПУЧКА В ЛІНІЙНОМУ ІНДУКЦІЙНОМУ ПРИСКОРЮВАЧІ ПРИ ЙОГО КОМПЕНСАЦІЇ ЕЛЕКТРОННИМИ ПУЧКАМИ

О.В. Федоровська, В.І. Маслов, І.М. Оніщенко

Вивчено динаміку сильнострумового протонного пучка в магнітному полі каспа та в однорідному магнітному полі дрейфової області за наявності в області каспа прискорюючого поля та двох типів електронних пучків (до і після каспа). Для вибраних параметрів пучків та магнітного поля показана неможливість прискорити протонний пучок щільністю понад 10^{12} см$^{-3}$ зі збереженням його поперечних розмірів та моноенергетичності.

УСКОРЕНИЕ СИЛЬНОТОЧНОГО ПРОТОННОГО ПУЧКА В ЛИНЕЙНОМ ИНДУКЦИОННОМ УСКОРИТЕЛЕ ПРИ ЕГО КОМПЕНСАЦИИ ЭЛЕКТРОННЫМИ ПУЧКАМИ

О.В. Федоровская, В.И. Маслов, И.Н. Онищенко

Изучена динамика сильноточного протонного пучка в магнитном поле каспа и в однородном магнитном поле дрейфовой области при наличии в области каспа ускоряющего поля и двух типов компенсирующих электронных пучков (до и после каспа). Для выбранных параметров пучков и магнитного поля показана невозможность ускорить протонный пучок плотностью большей 10^{12} см$^{-3}$ с сохранением его поперечных размеров и моноэнергетичности.